

NUMERICAL SIMULATION AND *IN VITRO* EXPERIMENTAL TEMPERATURE DISTRIBUTION ANALYSIS IN IRRADIATED TISSUE

Mioara PETRUS¹, Dan C. DUMITRAS²

In aplicațiile laser în medicina este foarte important să se aibă un control asupra temperaturii din tesutul iradiat. Temperaturile înalte duc la afectarea termică a tesutului înconjurător. Astfel, pentru a se studia efectul termic în tesut au fost iradiate în vitro amigdale de porc folosind un sistem laser cu CO₂ chirurgical, iar zona afectată termică a fost analizată cu ajutorul Tomografiei Optice Coerente (OCT). Pastrand aceeași parametri ai laserului cu CO₂ (putere, timp de expunere și diametru fascicul), s-au realizat simulări numerice 3D în Comsol folosind Metoda Elementelor Finite. Modelarea matematică a transferului de căldură în tesutul iradiat cu laser se face folosind ecuația Pennes de transfer a căldurii. Simulările numerice au fost comparate cu imaginile experimentale de OCT pentru optimizarea parametrilor laser. Cunoașterea distribuției de temperatură în tesutul iradiat cu radiație laser poate fi utilizată în stabilirea protocolelor terapeutice pentru un tratament cu laser mai eficient.

In treatments, that use laser radiation it is important to have a control of temperature, high temperature could lead to thermal damage in the surrounding tissue. Experimentally, porcine vocal cords were irradiated in vitro by a CO₂ laser surgical system and crater ablation images analyzed by an Optical Coherence Tomography (OCT). Using the same CO₂ laser parameters (absorption coefficient, power, exposure time, laser beam diameter), were realized in Comsol 3D simulation. The temperature response of tissue irradiation is governed by Pennes bio-heat equation. The numerical solutions are obtained by the Finite Element Method (FEM). This numerical method of temperature distribution modeling can also be used for extensive parametric studies in order to characterize the stability of various treatment parameters and would allow obtaining a faster and better simulation in laser treatment of biological tissues.

Keywords: laser irradiation, CO₂ laser, biological tissue, temperature distribution, bio-heat equation, numerical simulation

¹ Researcher, Department of Laser, National Institute for Laser, Plasma and Radiation Physics, Magurele, Bucharest, Romania. e-mail: mioara.petrus@inflpr.ro

² CS I, Department of Laser, National Institute for Laser, Plasma and Radiation Physics, Magurele, Bucharest, Romania; Prof. Faculty of Applied Sciences, University Politehnica of Bucharest, Romania

1. Introduction

Because of desirable features such as high precision, less blood loss and minimal invasiveness, carbon dioxide (CO_2) lasers are widely used as cutting tools [1, 2] in many medical fields. In treatments, that use laser radiation it is important to have a control of temperature, high temperature could lead to thermal damage in the surrounding tissue [1,2]. The deposition of laser energy in the tissue is not only a function of laser parameters such as wavelength, power density, exposure time, spot size, and repetition rate [1], it also depends on opto - thermal tissue parameters. To choose the treatment parameters properly and to predict the outcome of the photothermal effect, a reliable tissue model and simulation method is needed. Temperature is the governing parameter of all thermal laser- tissue interactions [2]. Depending on the tissue temperature, different effects are observed. For example, the denaturation of the enzymes and the looseness of the membranes occurs at $40-45^{\circ}\text{C}$; coagulation, necrosis and protein denaturation occurs around 60°C ; drying out occurs at 100°C ; carbonization occurs at 150°C , and, finally, pyrolysis and vaporization occurs at above 300°C [3]. Among those temperatures, 45°C is a characteristic temperature used frequently in photodynamic therapy. Increasing the tissue temperature to 100°C boiling of tissue water is induced. For continued heating of dehydrated tissue to about 400°C an initiated burning with the production of char tissue and smoke it is observed [1,2]. Therefore, for the purpose of predicting the thermal response, a model for the temperature distribution inside the tissue must be derived.

In this paper, the soft tissue model is used to predict the temperature distribution during CO_2 laser treatment. Finite element method (FEM) is applied for modeling of numerical simulation to predict the dynamic of temperature in human tissue using Pennes bioheat equation. The objective of this research is modeling the laser-tissue interaction, to optimize the effective parameters in order to understand optimal laser dosage and to prevent the tissue damage. Numerical simulations are compared with the OCT (Optical Coherent Tomography) images of the pig vocal cords irradiated zone by a CO_2 surgical system.

2. Mathematical model

To generate the finite element model we used the software Comsol Multiphysics [4]. This software provides all the elements needed to build the model, solve the problem and post-process the results. Solutions in simple cases (simple geometry, independent of temperature or uniform tissue properties) guides us to understand how the heat behave. The numerical solution relies on the Finite Element Method, in which the geometry studied is divided into a finite element mesh with computer software that makes it possible to numerically solve partial differential equations. Thus, instead of trying to solve a highly non-linear problem

on the entire geometry, an approximate solution is sought in each element. If this element is considerably small the physical problem is assumed to vary linearly. Numerical simulation helps us in obtaining the desired result according to the laser parameters and pathology [5,6]. The heating of tissue during laser ablation is modeled by the bioheat equation [6,7]:

$$\rho C \frac{\partial T}{\partial t} + \nabla(-k \nabla T) = \rho_b C_b \omega_b (T_b - T) + Q_{met} + Q_{laser} \quad (1)$$

where, ρ , C and k are the density, specific heat and thermal conductivity of the tissue, Q_{met} is the metabolic heat generation per unit volume, ρ_b , C_b are the density and the specific heat of blood, ω_b is the blood perfusion rate, T_b the temperature of arterial blood, T is the local tissue temperature and Q_{laser} (W/m³) is the heat source, or external heat source:

$$Q_{laser} = \mu_a I \quad (2)$$

where, μ_a (m⁻¹) is the absorption coefficient and I (W/m²) is the laser intensity.

The light absorption in the tissue was modeled as an exponential decay using Beer-Lambers law:

$$I = I_0 \exp(-\mu_a z) \quad (3)$$

where, $I_0 = \frac{P}{A}$ is the intensity of laser, A (m²) is the area of the tissue and

P (W) is the output power of the laser.

To accomplish our model we have made different stapes. The first step was to choose the geometry of the model, tissue sample being a cylinder. Then we have defined the physical properties and the boundary conditions as well as Q_{laser} . The external heat source is due to the absorption in the stained tissue, i.e. $Q_{laser} = 0$ everywhere except in the cylindrical subdomain representing the laser spot. The laser spot was considered as a cylindrical sub-domain, where heat source was confined. Boundary conditions depend on the particular problem and, the most usual case is a biological tissue irradiated from the outside and the laser light propagated in a direction perpendicular to the tissue. In this case continuity is commonly assumed, which means that the gradient of the temperature with respect to the coordinate affected by the boundary is zero ($\partial T / \partial x = 0$; $\partial T / \partial y = 0$; $\partial T / \partial z = 0$). Initial and boundary conditions can be set by using the steady-state temperature of biological tissue [5,6], $t = 0$, $T = T_b$, i.e., the initial temperature of the tissue is equal to the blood temperature. The initial temperature at $t = 0$, was set at 310.15 K (37 °C). The heat generation by metabolism and heat transfer by blood perfusion are constant in biological tissue [8-11]. The laser beam profile used in our experiments and numerical analysis was a Gaussian profile, which means that the concentration of energy focuses on its center section [12]. The spot

diameter $d = 800 \mu\text{m}$ of the laser is the same used in the experimental analysis and the absorption coefficient used is $\mu_a = 767 \text{ cm}^{-1}$ [3], which correspond to the absorption coefficient of $10.6 \mu\text{m}$ in soft tissue. Moreover, the following assumptions were adopted: thermal radiation emission at the tissue/air interface and reflection of laser light from the external surface of the cornea were disregarded; the thermo-optical parameters were considered to be constant during the process. The bioheat equation is solved for a single layer model of the soft tissue to predict the temperature distribution using CO_2 laser light source radiation burns at as steady state. The output is the real time temperature of the tissue. Plots of temperature changes with time can also be derived [11, 12].

Tabel 1

The optical and thermal properties for soft tissue used in numerical simulation

Parameters	Value
Specific heat of tissue - C	$3600 \text{ J/kg}^{\circ}\text{K}$
Density of tissue - ρ	1050 kg/m^3
Thermal conductivity tissue - k	$0.5 \text{ W/m}^{\circ}\text{K}$
Blood perfusion rate tissue - ω_b	0.0005 ml/s/ml
Arterial blood temperature - T_b	37°C (310.15 K)
Specific heat of blood - C_b	$4200 \text{ J/kg}^{\circ}\text{K}$
Density of blood - ρ	1000 kg/m^3
Heat coefficient transfer - h	$10 \text{ W/m}^2 \text{ K}$
Surrounding air temperature	23°C (296.15 K)

3. Experimental procedure

Porcine vocal cords were irradiated *in vitro* using a CO_2 laser surgical system (SP-25LA, China), in pulse regime with the maximum output power for laser system of 25 W [13]. The irradiation occur at 6 W, 14 W, 20 W and 24 W and exposure time of 100 ms. For a good positioning accuracy and reproducibility, the laser radiation is applied on vocal cords with a micromanipulator (Acuspot 711 Sharplan) under microscopic control and the laser beam had a Gaussian profile. For the experimental research were used porcine larynxes which were obtained from a local packing company, according with the EU standard. The thermal damage was analyze with a Thorlabs OCP930SR Spectral Radar OCT device and the OCT system used in our study is based on Fourier-Domain [14,15]. The refractive index of porcine vocal cords of $n = 1.39$ was taken into account for crater depth determination with OCT [15].

4. Results and discussions

4.1 Experimental results

Temperature dynamics during laser tissue ablation was studied experimentally by irradiation of larynx tissue with a CO₂ laser surgical system at different powers and different exposure times. Experimental analysis of the crater ablation is presented in Fig. 1 by the OCT images, which show the thermal damage in biological tissue after laser irradiation at different powers (6 W, 14 W, 20 W and 24 W) and an exposure time of 100 ms. It can be observed that the ablation volume and the thermal damage in the surrounding tissue increase with the power of the laser beam. The irradiation area is indicated by a bleak ring on the figures. The ablation crater has a conic shape, with an input aperture of about 800 μm diameter and a depth of ~ 0.64 mm at 14 W, 0.86 mm at 20 W and 0.92 W at 24 W, which is in accordance with the focal length of the laser beam focusing system ($f = 125$ mm) and with the laser beam divergence. At the lower power of the laser beam i.e., the 6 W, the irradiation effects are observed only as a necrosis zone there is no ablation crater in the tissue (see Fig. 1a.).

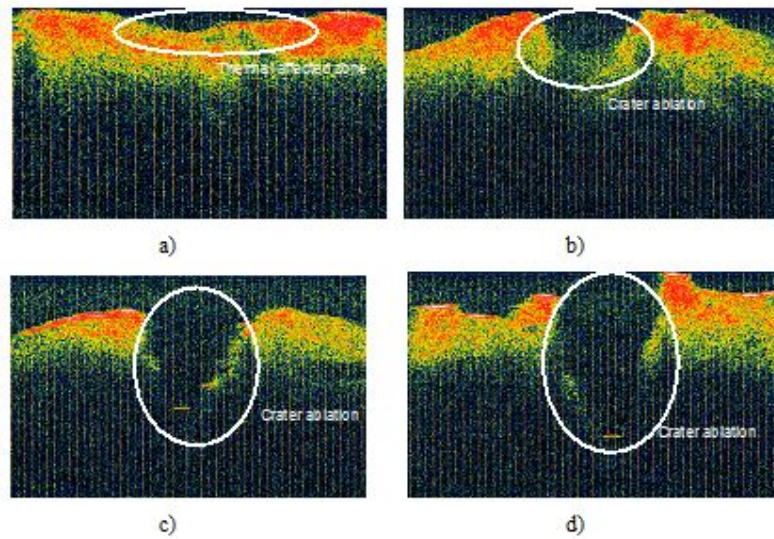


Fig. 1 OCT images of the crater ablation in porcine vocal cord using a CO₂ at $t_{\text{exp}} = 100$ ms at laser power: (a) $P = 6$ W, (b) $P = 14$ W, (c) $P = 20$ W, (d) $P = 24$ W

4.2 Numerical analysis results

During laser treatment it is very important to study the temperature rise in the laser irradiated wound area, and to evaluate the temperature in the surrounding tissues does not exceed the threshold of irreversible thermal damage.

Numerical analysis of 3D temperature distribution in CO₂ irradiated soft tissue was studied. For the numerical simulations were used the laser parameters used *in vitro* to ablate the tissue, the wavelength of 10.6 μm (CO₂ laser

wavelength), the corresponding absorption coefficient in the tissue, laser powers of 6 W, 14 W, 20 W and 24 W, an exposure of tissue to the laser beam of 100 ms and a laser beam with diameter of 800 μm . The tissue parameters used are presented in Table 1. The CO₂ laser has a small penetration depth in the tissue of 15 – 20 μm [1], and because of the small depth of penetration it was assumed that the irradiated tissue layer is homogeneous.

The computational models are simulated and presented in Fig. 2-5. Fig. 2-5 shows the three-dimensional temperature distribution in irradiated tissue at 6 W, 14 W, 20 W and 24 W at an irradiation time of 100 ms, and the temporal evolution of temperature with depth. At laser power of 6 W and exposure time of 100 ms the maximum temperature is 67⁰ C (see Fig. 2). At this temperature there is no laser ablation in the tissue, is presented coagulation, necrosis and protein denaturation, the tissue is thermal affected, and this can be seen also in the OCT image (see Fig. 1(a)). By increasing the laser power, the increased temperature in the tissue, at 107⁰ C tissues drying (see Fig. 3) and at 137⁰ C and 160⁰ C tissues carbonization (see Fig. 4 and 5). From the numerical simulation at 14 W, 20 W and 24 W can be seen that the temperature exceeds 100⁰ C with the ablation crater that is present even in the OCT images (see Fig. 1) with the crater ablation irradiation results.

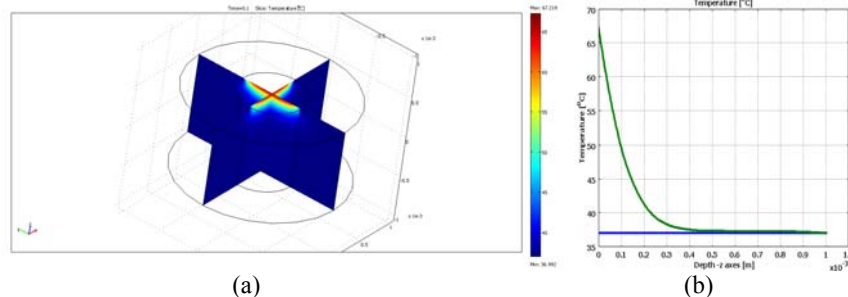


Fig. 2 Temperature distribution in tissue irradiated at $P = 6$ W and $t_{\text{exp}} = 100$ ms: (a) 3D temperature distribution; (b) temporal evolution of temperature with depth, $T(x = 0, y = 0, z, t = 100 \text{ ms})$

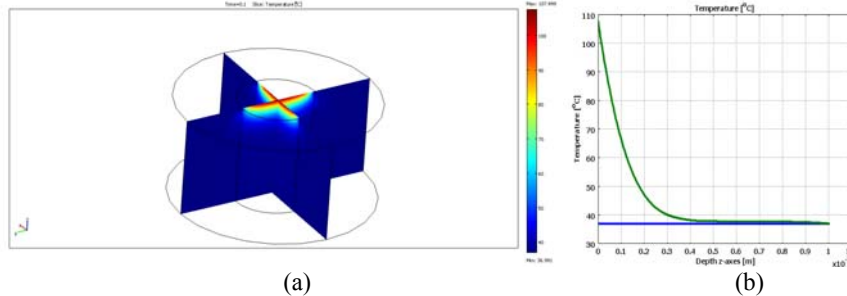


Fig. 3 Temperature distribution in tissue irradiated at $P = 14$ W and $t_{\text{exp}} = 100$ ms: (a) 3D temperature distribution; (b) temporal evolution of temperature with depth, $T(x = 0, y = 0, z, t_{\text{exp}} = 100 \text{ ms})$.

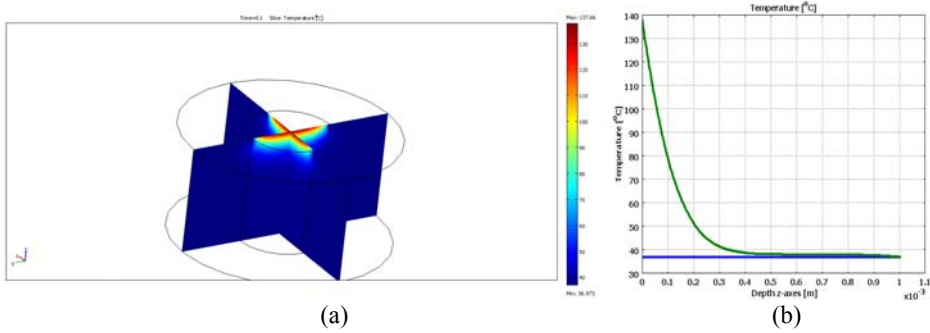


Fig. 4 Temperature distribution in tissue irradiated at $P = 20$ W and $t_{\text{exp}} = 100$ ms: (a) 3D temperature distribution; (b) temporal evolution of temperature with depth, $T(x = 0, y = 0, z, t_{\text{exp}} = 100$ ms).

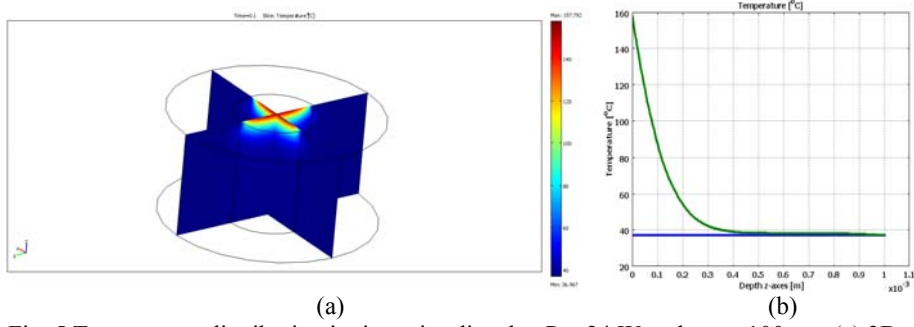


Fig. 5 Temperature distribution in tissue irradiated at $P = 24$ W and $t_{\text{exp}} = 100$ ms: (a) 3D temperature distribution; (b) temporal evolution of temperature with depth, $T(x = 0, y = 0, z, t_{\text{exp}} = 100$ ms).

The temperature evolution in time in irradiated tissue at 6 W, 14 W, 20 W and 24 W is presented in Fig. 6. It can be observed that the temperature tends to a constant steady-state value for the irradiation time longer than 1 s. Therefore, the exposure time is an important parameter in the medical laser applications, especially for very short exposure time. As one can observe, the time needed to reach the constant steady-state value temperature is independent of the optical source power. However, the value of the constant temperature depends on the laser power. Due to this increase in the tissue temperature; one must optimize with a high accuracy the two laser parameters: the exposure time and the power of the laser.

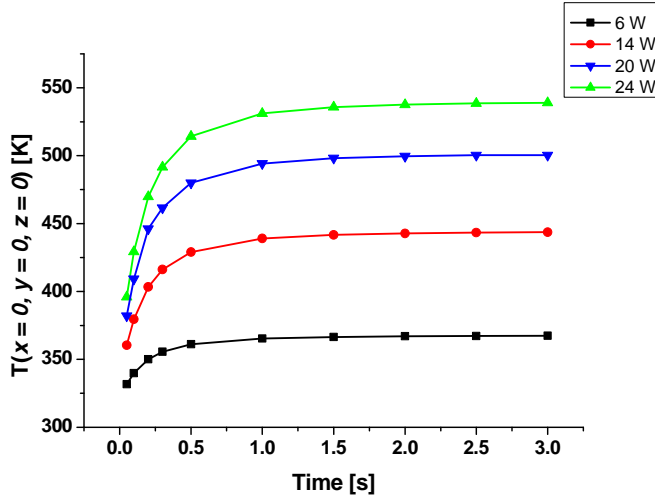


Fig. 6 Temporal evolution of temperature at laser impact point $T(x = 0, y = 0, z = 0)$, different laser powers: 6 W, 14 W, 20 W and 24 W and an irradiation time of 100 ms

4. Conclusions

In this work, a 3D numerical approach for the bio-heat equation has been presented and the numerical procedure has been analyzed. The model was applied to the irradiated soft tissue and the results compared with the experimental OCT dates. We simulate the temperature evolution in biological tissue using the wavelength of $10.6 \mu\text{m}$ which is strongly absorbed by the water and has a small penetration depth in biological tissue of $\sim 15 - 20 \mu\text{m}$ [1]. In this case, the tissue parameter homogeneity remains constant over time (C, k, ρ). The numerical simulations are in good agreement with the OCT images obtained after *in vitro* irradiation of pig vocal cords.

The results obtained from the study reveal the important parameters, which significantly affect the thermal response of soft tissue, as exposure duration, power, wavelength of the beam, as well as the area and type of the tissue. The exposure time is an important parameter in the medical laser application and an increase of the temperature in the tissue after a long exposure and propagation of the heat in the surrounding tissue leads to thermal damage.

The numerical method of temperature distribution modeling can also be used for extensive parametric studies in order to characterize the stability of various treatment parameters and would allow obtaining a faster and better simulation of laser treatment of biological tissues. Solving the bioheat equation numerically, allows obtaining useful information for analysis of different laser

surgical techniques. The present model could serve as a good tool to predict temperature distribution in tissues under laser irradiation.

R E F E R E N C E S

- [1] *R.H. Ossoff, L. Reinisch*, Chapter 12: Laser Surgery: Basic Principles and Safety Considerations, C.V. Mosby Company, St. Louis 1986.
- [2] *M.H. Niemz*, Laser-tissue interactions, Fundamentals and Applications, Third Enlarged Edition, Springer 2007.
- [3] *R. Steiner*, Laser and IPL Technology in Dermatology and Aesthetic Medicine, Chapter: Laser-tissue interactions, Springer-Verlag Berlin Heidelberg 2011.
- [4] *G. Demésy, L. Gallais, M. Commandré*, Tridimensional multiphysics model for the study of photo-induced thermal effects in arbitrary nano-structures, *J. Europ. Opt. Soc. Rap. Public.* 11037, **vol 6**, 2011.
- [5] *F. Rossi, R. Pini, L. Menabuoni*, 3D Simulation and Experimental Comparison of Temperature Dynamics in Laser Welded Cornea, *Proceedings of the COMSOL Users Conference*, Milano 2006.
- [6] *M.J. Rivera, J.A. Lopez Molina, M. Trujillo, V. Romero-Garcia, E.J. Berjano*, Analytical validation of Comsol Multiphysics for theoretical models of radiofrequency ablation inculding the hyperbolic bioheat transfer equation, *Engineering in medicine and Biology Society (EMBC), Annual International Conference of the IEEE* 2010.
- [7] *H.H. Pennes*, Analysis of tissue and arterial blood temperature in the resting human fore-arm, *Journal of Applied Physiology*; **vol. 1**, 1948, pp. 93 – 122.
- [8] *S. Maruyama, J. Okajima, A. Komiya, H. Takeda*, Estimation of Temperature Distribution in Biological Tissue by Using Solutions of Bioheat Transfer Equation, *Heat Transfer—Asian Research*; **vol. 37**, no. 6, 2008, pp. 375-388.
- [9] *P.K. Gupta, J. Singh, K.N. Rai*, Numerical simulation for heat transfer in tissue during thermal therapy, *Journal of Thermal Biology*; **vol. 35**, 2010, pp. 295-301.
- [10] *F. Fanjul-Velez, O.G. Romanov, J.L. Arce-Dego*, Efficient 3D numerical approach for temperature prediction in laser irradiated biological tissues, *Computers in Biology and medicine*; **vol. 39**, 2009, pp: 810-817.
- [11] *J. Zhou, Y. Zhang, J.K. Chen*, An axisymmetric dual-phase-lag bioheat model for heating of living tissues, *International Journal of Thermal Sciences*; **vol. 48**, 2009, pp. 1477-1485.
- [12] *Q.M. Luong, S.D. Dams*, The Light Distribution In Skin Of A 976nm Laser Diode Using Different Parameter Sets In Monte Carlo Simulations, *Koninklijke Philips Electronics N.V.* 2009.
- [13] *M. Petrus, E.M. Carstea, D.C.A. Dutu, D.C. Dumitras*, Optical coherence tomography monitoring of laser ablation processes in ENT tissues, *J. of Optoelectronics and Adv. Mat.*, **vol. 13**, no.7-8, 2011, pp. 776-780.

- [14] *H. Wisweh, U. Merkel, A.K. Huller, K. Luerben, H. Lubatschowski*, Optical coherence tommography of vocal fold femtosecond laser microsurgery, Therapeutic Laser Applications and Laser-Tissue Interactions III, Proc. SPIE, **vol. 6632**, 2007, pp. 527-533.
- [15] *R. Leitgeb, W. Drexler, A. Unterhunber, B. Hermann, T. Bajraszewski, T. Le, A. Stingl, A. Fercher*, Ultrahigh resolution Fourier domain optical coherence tomography, Optics Express; **vol. 12**, no. 10, 2004, pp. 2156-2165.